Article

Cell*Press*

Live Imaging of Axolotl Digit Regeneration Reveals Spatiotemporal Choreography of Diverse Connective Tissue Progenitor Pools

Joshua D. Currie,[1,2,*] Akane Kawaguchi,[1] Ricardo Moreno Traspas,[1] Maritta Schuez,[1] Osvaldo Chara,[3,4] and Elly M. Tanaka[1,2,5,6,*]

[1]DFG Research Center for Regenerative Therapies, Technische Universität Dresden, Fetscherstrasse 105, 01307 Dresden, Germany
[2]Max Planck Institute of Molecular Cell Biology and Genetics, Pfotenhauserstrasse 108, 01307 Dresden, Germany
[3]Center for Information Services and High Performance Computing (ZIH), Technische Universität Dresden, 01062 Dresden, Germany
[4]Systems Biology Group (SysBio), Instituto de Física de Líquidos y Sistemas Biológicos (IFLySIB), CONICET, Universidad Nacional de La Plata (UNLP), B1900BTE La Plata, Buenos Aires, Argentina
[5]Present address: Research Institute for Molecular Pathology (IMP), Campus-Vienna-Biocenter 1, 1030 Vienna, Austria
[6]Lead Contact
*Correspondence: josh.currie@crt-dresden.de (J.D.C.), elly.tanaka@imp.ac.at (E.M.T.)
http://dx.doi.org/10.1016/j.devcel.2016.10.013

SUMMARY

Connective tissues—skeleton, dermis, pericytes, fascia—are a key cell source for regenerating the patterned skeleton during axolotl appendage regeneration. This complexity has made it difficult to identify the cells that regenerate skeletal tissue. Inability to identify these cells has impeded a mechanistic understanding of blastema formation. By tracing cells during digit tip regeneration using brainbow transgenic axolotls, we show that cells from each connective tissue compartment have distinct spatial and temporal profiles of proliferation, migration, and differentiation. Chondrocytes proliferate but do not migrate into the regenerate. In contrast, pericytes proliferate, then migrate into the blastema and give rise solely to pericytes. Periskeletal cells and fibroblasts contribute the bulk of digit blastema cells and acquire diverse fates according to successive waves of migration that choreograph their proximal-distal and tissue contributions. We further show that platelet-derived growth factor signaling is a potent inducer of fibroblast migration, which is required to form the blastema.

INTRODUCTION

A key question of limb regeneration is how cells are recruited out of diverse, mature tissues to form a mass of progenitors called the blastema that produces a new skeleton appropriate to the missing limb segments (for review see Tanaka, 2016). Among the mature tissues that provide cells to the blastema, one critical cell source are lateral plate mesoderm (LPM)-derived connective tissue cells. These cells contribute at least 40% of the cells found in a mid-bud blastema and are responsible for regenerating the new skeleton (Dunis and Namenwirth, 1977; Kragl et al., 2009; Muneoka et al., 1986). Indeed, connective tissue-derived cells

harbor positional memory and positional identity, properties that are necessary to appropriately regenerate only the missing portion of the limb (Carlson, 1974; Kragl et al., 2009; Nacu et al., 2013; Rollman-Dinsmore and Bryant, 1982).

Limb connective tissue encompasses many related cell types including the skeleton, tendons, dermal fibroblasts, and fibroblastic cells that surround the skeleton (periskeletal), blood vessels (pericytes), and muscles (fascia). It is currently unknown which of these subtypes represent the major source of blastema cells. Previous grafting experiments onto irradiated hosts showed that dermal tissue is competent in making new skeletal tissue (Dunis and Namenwirth, 1977). It has, however, not been clear whether these dermal cells constitute the only connective tissue subtype that contributes significantly to normal regeneration or whether other subtypes may make similar or distinct contributions to the regenerate. Chondrocytes and bone tissue have been studied in various grafting experiments, and the conclusions about their participation has ranged from no participation to a significant number of participating cells (Cameron and Hinterberger, 1984; McCusker et al., 2016; Muneoka et al., 1986). Finally, the fate of pericytes, a cell type that has been identified as contributing to multiple tissue types upon injury in mammals, has not been described at all in salamander limb regeneration (Cappellari and Cossu, 2013). In addition to uncertainty about the relevant cell subtypes, it is unknown whether regeneration selects subsets of cells within a given compartment, or whether it wholesale recruits many cells from a tissue. Also unresolved is whether cells migrate from long distances toward the amputation plane to seed the blastema or whether only those cells adjacent to the amputation participate. Finally, it is unknown whether the recruitment of cells from the mature tissue occurs only in the first few days after limb amputation or whether it continues over an extended period of time.

This uncertainty about the cell source of the blastema has hindered a molecular dissection of blastema formation. For example, since prospective blastema-forming cells could not be isolated from the mature limb, gene expression studies have focused on comparing whole adult tissue with blastema tissue (Monaghan et al., 2009) (Knapp et al., 2013; Stewart et al.,

2013). It is, however, already known that a large fraction of cell mass at the amputation plane does not contribute to the blastema, since tracking of muscle fibers showed that they do not participate in axolotl limb regeneration (Sandoval-Guzman et al., 2014). Therefore, comparing whole limb tissue with blastema cells has been of limited use for identifying transcripts that are truly upregulated in blastema-forming cells, since the representation of prospective blastema cells in the adult tissue differs from the representation of their descendants in the blastema. Furthermore, it has been difficult to prove changes in gene expression in blastema-forming cells, since they have not been identified histologically or molecularly.

The identification and tracking of blastema cell precursors in the mature tissue is therefore an essential requirement for a mechanistic understanding of blastema formation. Until now, a number of limitations have prevented the tracking of connective tissue cells from their tissue of origin into the blastema, and further into the regenerated structure. Connective tissue is a diverse set of tissue types, and promoter elements often express in multiple compartments. The complexity and size of the limb as a macroscopic tissue is daunting, and becomes even more challenging during regeneration when cells are highly dynamic. The upper or lower limb region of a larval animal has a diameter of 2 mm, severely limiting the ability to follow cells through regeneration. An ideal system to address cell contribution to regeneration would (1) resolve multiple tissue compartments, (2) label individual cells within various compartments, and (3) resolve cells throughout the process in individual animals over time.

To address these needs, we created connective tissue-labeled multicolor "brainbow" (Livet et al., 2007) axolotls and adapted long-term imaging of digit tip regeneration to acquire a cellular view of skeletal regeneration. These data have allowed us to define the role of each connective tissue cell type, and the cell behaviors that govern digit blastema formation. Two cell types, chondrocytes and pericytes, showed limited contributions to digit regeneration, while dermal fibroblasts and periskeletal cells contributed to multiple connective tissue types and showed a larger degree of contribution to the regenerate. Dermal fibroblasts and periskeletal cells had different migratory dynamics that influenced their contribution to skeletal and soft connective tissue. Even within a given tissue compartment, the distance from the amputation plane plays a role in determining the degree and type of contribution. The source cells entered the blastema through sequential waves of migration at early and late times during regeneration to bias contribution toward regenerated skeleton and periskeleton for early-arriving progenitors, or lateral soft connective tissue structures such as dermis and periskeletal compartments for late-arriving cells.

We then queried molecular factors that influence cell recruitment into the blastema. We screened an ex vivo connective tissue cell culture for extracellular factors that promote migration after scratch wounding and identified platelet-derived growth factor (PDGF) BB as a stimulator of cell migration. In vivo inhibition of PDGF receptor (PDGFR) signaling blocked the migration of soft connective tissue cells and prevented blastema formation. This work has identified how digit blastema cells are made in space and time and has established a system for understanding the cell biology of blastema formation, the cellular process that defines regeneration capability.

RESULTS

Overview of Digit Tip Regeneration in Limbow Transgenic Axolotls

To determine which connective tissue cells migrate into the blastema and their contribution to the regenerated skeleton, we aimed to perform live imaging of digit tip regeneration. To facilitate cell tracking, we created stable transgenic axolotls that express multicolor "brainbow" cassettes (Figure S1A) (Livet et al., 2007). Upon Cre-mediated recombination, these transgenes generate combinatorial expression of fluorescent proteins, endowing cells with different, heritable color identities. We used a tamoxifen-inducible Cre recombinase driven by the ubiquitous CAGGS promoter that induced random patterns of ubiquitous, multicolored fluorescence (Khattak et al., 2013). To specifically label connective tissue within the limb, we implemented embryonic transplantation of LPM from the double transgenic animals into nontransgenic hosts (Figure S1B) (Kragl et al., 2009). Tamoxifen was administered to clonally label mature cells after limb development had finished (Figure S1C). Cells were followed for 2 weeks prior to amputation to ensure that recombined colors were stable. We termed these animals "Limbow" animals. Since we expected noncoherent clones, we were not confident to use the obtained color diversity to perform retrospective clonal analysis. Rather, the color diversity was used to identify individual cells in a given starting tissue and to track them by successive live imaging. The added benefit of the longitudinal imaging strategy over retrospective analysis was that we could observe how, when, and from where cells transitioned from mature tissue into the regenerative blastema.

The axolotl digit tip contains multiple, discernible connective tissue subcompartments, yet its small size and transparency allowed us to collect image stacks encompassing the entire digit volume to follow individual cells over time during regeneration (Figure S1D). The architecture of compartments in the fingertip such as the skeletal core, tendons, and blood vessels had a stereotypical arrangement in three dimensions so that cell types could be partitioned by morphology and location in live images (Figures 1A, 1A′, and 1C′). The uninjured digit skeleton of these stage animals contained calcein-stainable, calcified sections but these calcified segments were removed after amputation either manually or by a natural tissue-clearing process. Therefore the amputation plane consisted of a core of cartilage, surrounded laterally by encompassing periskeletal cells, blood vessel-associated pericytes, and dermal fibroblasts (Figures 1A′ and 1C′). The distal phalanx lacked muscle, which helped to reduced tissue complexity and light diffraction. To track cells, we collected an image stack covering the entire depth of the digit every 24 hr to reliably re-identify cells in consecutive images (Figures S1C and S1D). Axolotls have extremely large cells and a slow cell cycle, with the fastest cell-cycle length observed being 24 hr (Rodrigo Albors et al., 2015). Additionally we found that the extent of cell rearrangements was slow enough that imaging every 24 hr was sufficient to re-identify cells between successive images. Figures 1B–1G (see also Movie S1) presents selected images from a time series to provide a first overview of different morphological stages of digit regeneration. The images in Figures 1, S1A, and S1B, and Movie S1 show maximum-intensity projections of ten 2-μm sections out of an
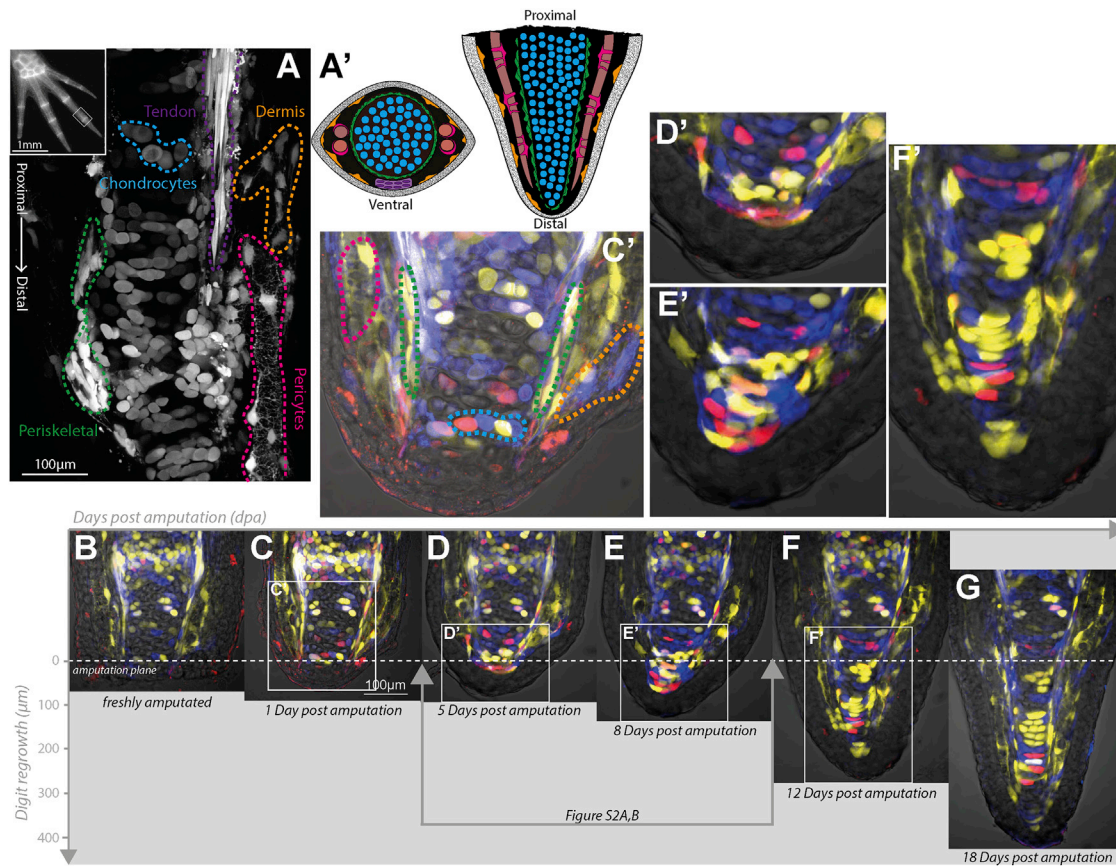
Figure 1. An Overview of Digit Connective Tissue Subtypes and Stages of Regeneration

(A) Inset: low-magnification view of Limbow larval hand visualized in a single fluorescent channel. Box marks a representative region that is amputated and imaged daily for 18 days. Main panel: connective tissue compartments can be distinguished within the digit tip by morphology and spatial orientation. B/W, single-channel confocal image of a converted Limbow digit delineates the different cell types. Image represents maximum projection of several z planes, and due to the conversion a subset of the digit cells are labeled in this sample. A ventral line of tendons (purple dashed outline) runs alongside a cartilaginous core of chondrocytes (blue) surrounded by periskeletal cells (green). Pericytes (pink) enwrap a blood vessel that runs lateral to the skeleton (see also Figure S3). The stromal space between cartilage and epidermis are occupied by dermal fibroblasts (orange).

(A′) The schema shows the overall arrangement of different cell types in the digit. Colors correspond to cell types in (A). Cross-section (left) and longitudinal view (right).

(B–G) Representative stages of Limbow digit tip regeneration. (B) Freshly amputated digit prior to epidermal wound healing. (C) Twenty-four hours after amputation, epidermis has covered the wound, but no connective tissue covers the cartilage core. (C′) Zoomed image of (C) that is color annotated to indicate the different cell types in the stump tissue before regeneration. (D) By 5 dpa, a layer of flattened connective tissue cells has covered the severed cartilage surface. (D′) Zoomed image of (D) showing first mesenchymal cell layer that overlays the cartilage. Cells are flattened along the PD axis, and show evidence of protrusive activity. (E) By 8 days, a blastema containing connective tissue-derived cells is visible beyond the amputation plane. (E′) Zoomed image of (E) showing that cells beyond the amputation plane at this stage have a rounded morphology. (F) By day 12, new tissue boundaries become visible in the regenerate, marking a transition phase whereby differentiation is happening. (F′) Zoomed image of (F) showing tissue organization, including laterally elongated cartilage cells in the core, surrounded by periskeletal cells elongated along the PD axis, and with pericytes enwrapping blood vessels further laterally on the left side. (G) The regenerate has continued to expand by day 18 toward the original tissue scale.

See also Figures S1 and S2.

entire 80-μm z stack and therefore represent the cells found in a 20-μm section of the digit. Within 24 hr of amputation, epidermal cells, visible in the bright field, had covered the wound surface but the terminus of amputated cartilage appeared similar to freshly amputated cartilage, suggesting that connective tissue from lateral tissues had not yet migrated centrally (Figures 1B, 1C, and 1C′). This observation is consistent with a time course of whole-mount, triploid skin-transplanted limbs (Gardiner et al., 1986). By 5 days post amputation (dpa), a thin layer of oblong cells flattened along the proximal-distal (PD) axis had

formed over the cut end of the cartilage (Figures 1D and 1D′). By 8 dpa, a number of cells beyond the amputation plane had accumulated, with the cells at the tip having a rounded but oblong morphology (Figures 1E and 1E′). By 12 dpa, the regenerated structure had increased in cell number and was cone-shaped. A clear central core had formed a seamless interface with the stump cartilage, suggesting condensation of cartilage at the base of the blastema (Figures 1F, 1F′, and S2C). Indeed, immunostaining of the regenerating digit at 10 dpa showed abundant SOX9⁺ chondrocytes in this core skeleton
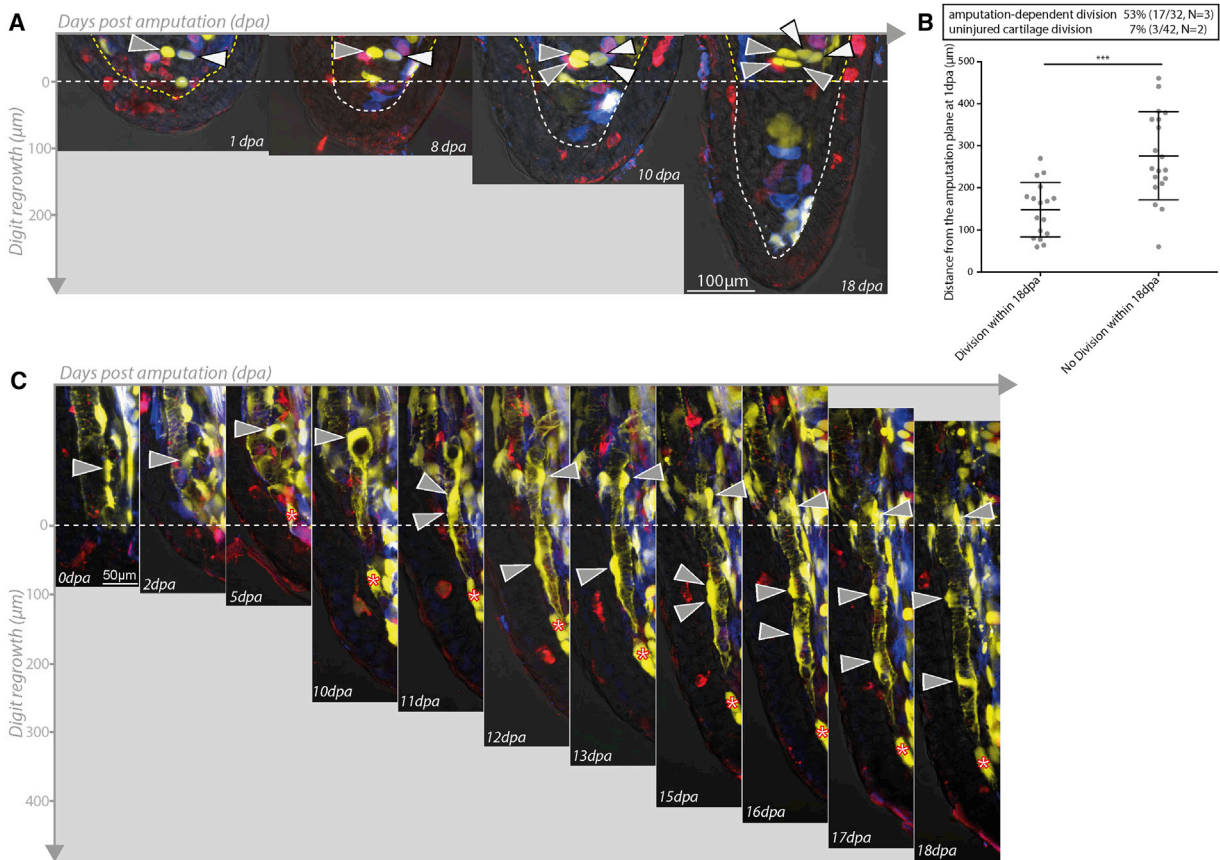
Figure 2. Restricted Participation of Chondrocytes and Pericytes during Digit Regeneration

(A) Chondrocytes near the amputation plane respond to injury by undergoing division, but do not enter the blastema or contribute to regenerated structures. Two chondrocytes near the amputation plane (white and gray arrowheads) each undergo a division by 10 dpa, but do not mobilize into the blastema. The amputation plane is indicated as a yellow dashed line and the mesenchymal blastema as a white dashed line.

(B) During regeneration, 53% of chondrocytes behind the amputation plane underwent cell division during the first 18 days of regeneration (17/32 cells, n = 3 animals) compared with 7% of chondrocytes in unamputated digits over the same time period (3/42 cells, n = 2 animals; ***p < 0.001, Mann-Whitney nonparametric). The proliferative response of chondrocytes is dependent on their distance from the amputation plane (p < 0.001, Mann-Whitney nonparametric). The majority of clones only underwent a single division over 18 days (one division 15/17, two divisions 2/17). Error bars represent SD.

(C) Pericytes (gray arrowheads) near the amputation plane reorganize along blood vessels and enter the blastema at late time periods (11 dpa), undergoing divisions (11 and 15 dpa) behind the amputation plane to leave sisters behind before migrating further along vessels into the regenerate. Red asterisks indicate a similarly colored dermal cell.

See also Figure S3.

(Figure S2D). Laterally the blastema contained cells elongated along the PD axis, with morphology resembling pericytes (Figure 1F′, yellow, left), and other cells with a more fibroblastic, lamellar shape suggestive of nascent dermal fibroblasts (Figure 1F′, yellow/blue, right). These data indicated that significant organization into the different tissue layers had happened between 8 and 12 dpa. Further growth of the regenerate was evident at 18 days, which maintained the essential tissue architecture. At day 18, the last day of data collection, the digit had substantially regenerated its length, but no calcified bone was yet detectable. Therefore, these experiments do not address the source of calcified bone during digit regeneration. Based on these tissue-scale morphologies, we divided regeneration into three phases, "early" (days 4–8), "middle" (days 9–11), and "late" (days 12–18). These stages correspond well to morphological stages observed during upper limb regeneration

(Bryant et al., 2002), validating the digit tip as an excellent model to observe connective tissue appendage regeneration.

Connective Tissue Cell Types with No or Limited Participation in Regeneration: Chondrocytes and Pericytes

We next sought to understand which cell types contribute to the blastema. This required tracking a single cell over the course of digit regeneration, which we defined as the first 3 weeks post amputation. Each clone was categorized based on its starting compartment to create a collection of cell behaviors associated with a certain source tissue type. Figures 1, 2, 3, 4, 5, and 6 show selected planes of image volumes in which the cell of interest is clearly identifiable. The 3D information in the complete stacks was used to distinguish the cell and its descendants from other cells entering the vicinity that might have similar color identities.
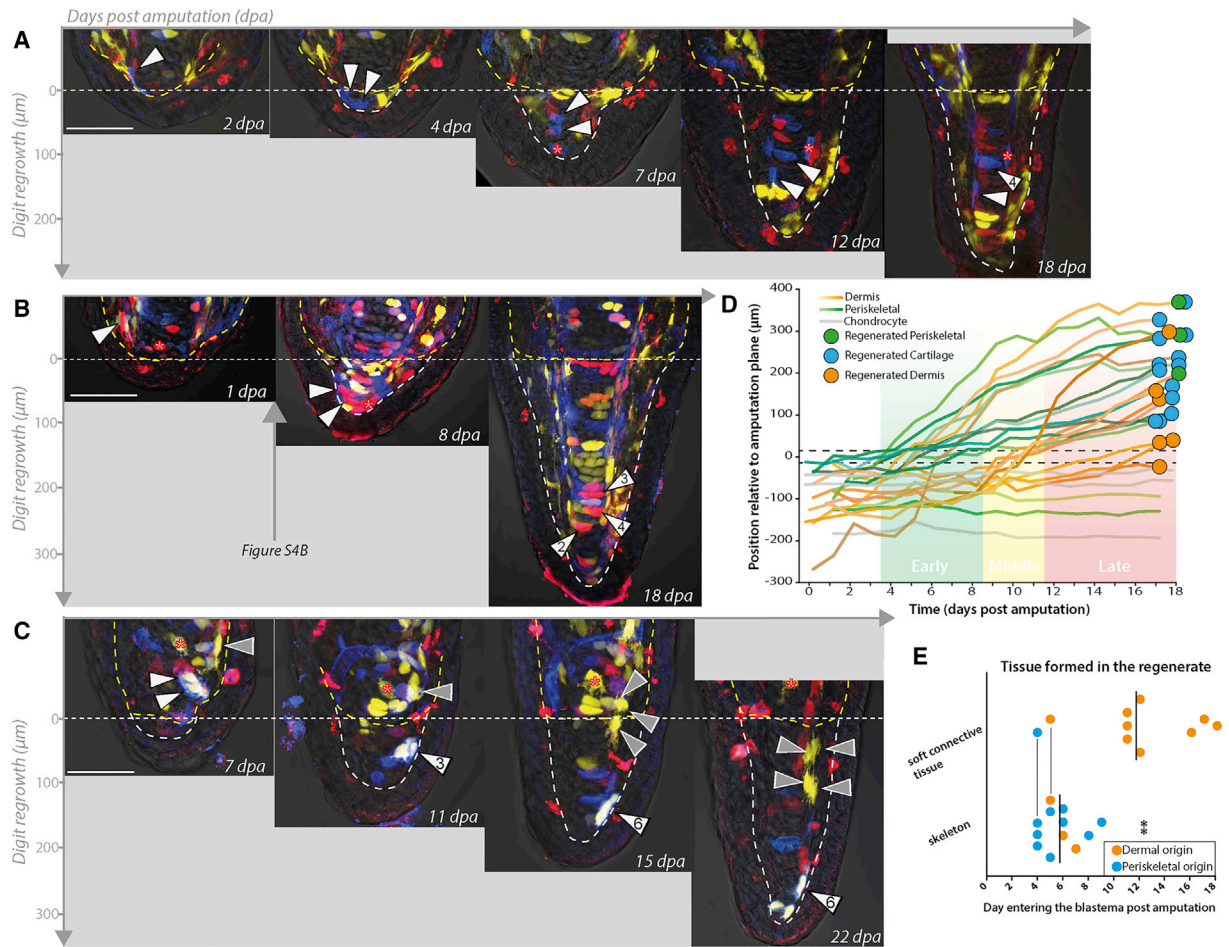
Figure 3. Early-Migrating Periskeletal and Dermal Fibroblasts Contribute to Skeletal Tissue, while Late-Migrating Dermal Fibroblasts Form Lateral Soft Connective Tissue

(A) A periskeletal cell close to the amputation plane (white arrowheads) enters the blastema early. One daughter contributes to forming cartilage while the elongated daughter forms a periskeletal cell.

(B) A dermal fibroblast close to the amputation plane (white arrowheads) has entered the blastema during the early phase and makes skeleton.

(C) Two dermal clones, one far from the amputation plane (gray arrowheads) and another closer pair (white arrowheads) enter the blastema at 15 and 10 dpa, respectively. The middle migrating clone reaches the distal tip while the late-arriving clone forms newly regenerated dermis in proximal regions of the regenerate by 22 dpa. Scale bars indicate 100 μm. Red asterisks indicate similarly colored clones. Horizontal dashed lines indicate the amputation plane. Outlining dashed lines indicate mesenchymal tissue.

(D) Traces documenting distal cell migration over time of three different connective cell derivatives, and their ultimate fate outcome, denoted as colored dots at end of the track (see also lineage trees in Figure S4A). Single cells are tracked at the beginning. If a cell divides, the trace tracks the PD mean distance of the clone relative to the amputation plane. Periskeletal cells (green tracks) migrate from close to the amputation plane, cross the amputation plane at early time points, and form regenerated periskeleton or cartilage. Bipotent clones were observed. Dermal cells (orange traces) migrate from a larger range of distances behind the amputation plane. Some cross the amputation plane in the early phase, while others cross during the late phase. Some dermal cells move distally, but do not end up crossing the amputation plane. Cells could contribute to dermis, cartilage, or periskeleton.

(E) Early-entering cells are biased to form skeleton and late cells are biased to form soft connective tissue. Periskeletal and dermal fibroblasts are plotted together based on when (dpa) the cell crosses the amputation plane (n = 22 of which dermal = 12, periskeletal = 10; n = 4 animals; **p < 0.005, Mann-Whitney nonparametric). Colored points indicate the tissue origin of the tracked cell. Bolded vertical lines indicate mean (5.75 ± 1.6 dpa for skeletally biased cells and 11.7 ± 4.6 dpa for soft connective tissue-biased cells). Vertical lines between points denote multipotent clones that formed both skeletal and soft connective tissue cells.

See also Figure S4.

We tracked four cell types: chondrocytes, pericytes, periskeletal cells, and dermal fibroblasts. We first describe the trajectories of chondrocytes that showed the most limited behavior. Chondrocytes were identified based on their spherical morphology, cell spacing, and location within the cartilaginous core of digit tip (Figure 2A). After amputation, within the field of imaging (approximately 700 × 700 μm² area), we observed a large increase in the number of dividing chondrocytes compared with those in uninjured digits (Figures 2A and 2B). Within the 18 days of observation, 53% of chondrocytes within 500 μm of
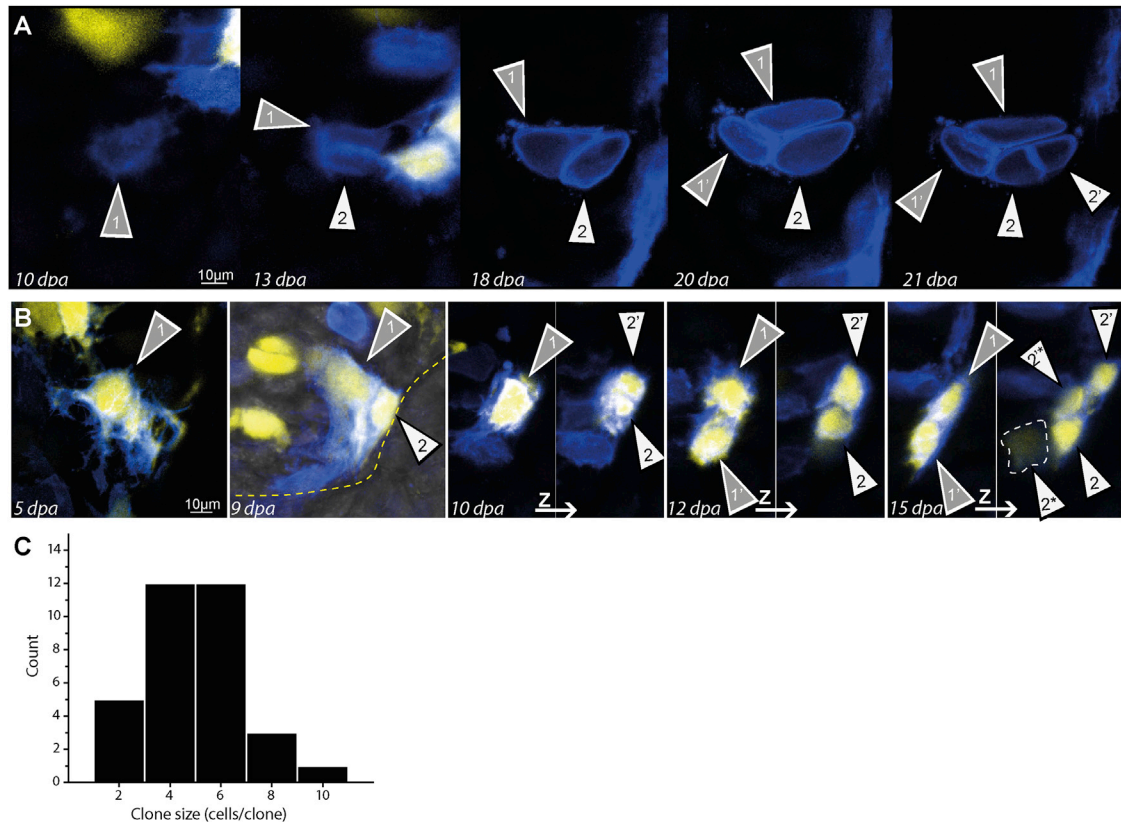
Figure 4. Dermal and Periskeletal Cell Proliferation during Regeneration

(A) Late-stage regeneration cartilage clone derived from a periskeletal cell undergoing proliferation.

(B) Dermal cell clone entering the blastema at 9 dpa undergoes several rounds of proliferation to generate a clone of six cells. Panels at 10, 12, and 15 dpa show multiple z projections to visualize all clone cells. Dashed line at 15 dpa indicates a clone cell at a deeper z plane. White and grey arrowheads indicate individual sister cells and their progeny over time.

(C) Histogram of clone sizes reflecting a relatively normal size distribution of clones at day 18 (indeed, normality cannot be rejected: Shapiro-Wilk test and Kolmogorov-Smirnov test, p = 0.2401 and p = 0.41669, respectively). Clones deriving from dermal and periskeletal cells were included (n = 33 cells, n = 6 animals).

the amputation plane underwent a cell division whereas in uninjured digits only 7% of cells underwent proliferation. The proliferative response behind the amputation plane usually involved a single division within the first 3 weeks of regeneration, and the likelihood of division was dependent on the proximity to the amputation plane (Figure 2B). Chondrocytes lacked any evidence of migration, and as their proliferation was limited we never observed a contribution of chondrocytes to the regenerated skeleton beyond the amputation plane (n = 15). Thus chondrocytes do proliferate in response to amputation but do not mobilize into the blastema.

We next characterized the fate of perivascular cells that were ubiquitously spread along blood vessels with intricate ramifications, and which we refer to as pericytes (Cappellari and Cossu, 2013). Their morphology was distinguishable from endothelial cells based on discontinuous membrane tendrils wrapping across the vessel with a protruding cell body, in contrast to the even illumination seen for fluorescently labeled endothelial cells (Figure S3). During regeneration, pericytes did not migrate into the blastema at early time points. Instead, migration occurred along vessels starting at 7–9 dpa only after endothelial cells (visualized by bright field, Figure S3C) first entered the blastema (Figure 2C).

We observed cell division of pericytes at or behind the amputation plane leaving a cell behind before a descendant migrated along vessels into the regenerate. Proliferation continued within the regenerate to create pericytes at regular intervals along regenerated vessels. Among the clones that we could track completely, we did not observe pericytes contributing to other tissues (n = 12).

Periskeletal and Dermal Fibroblasts Build the Regenerating Skeleton

Given the unipotency of chondrocytes and pericytes, we hypothesized that fibroblastic cells would be a major contributor to the regenerated digit, consistent with previous data (Dunis and Namenwirth, 1977). We subdivided such cells into two categories, periskeletal cells that surrounded the cartilage/joint structures and loose dermal fibroblasts that existed either directly under the epidermis or in the stromal space between epidermis and cartilage. We measured the location of the cells day by day, and noted proliferation as well as differentiation into the different cell types. These observations are summarized as cell tracks plotted as the distance from the amputation plane over time (Figure 3D). Since individual cells founded clones, the tracks start out tracing a single cell and when a cell divided, the
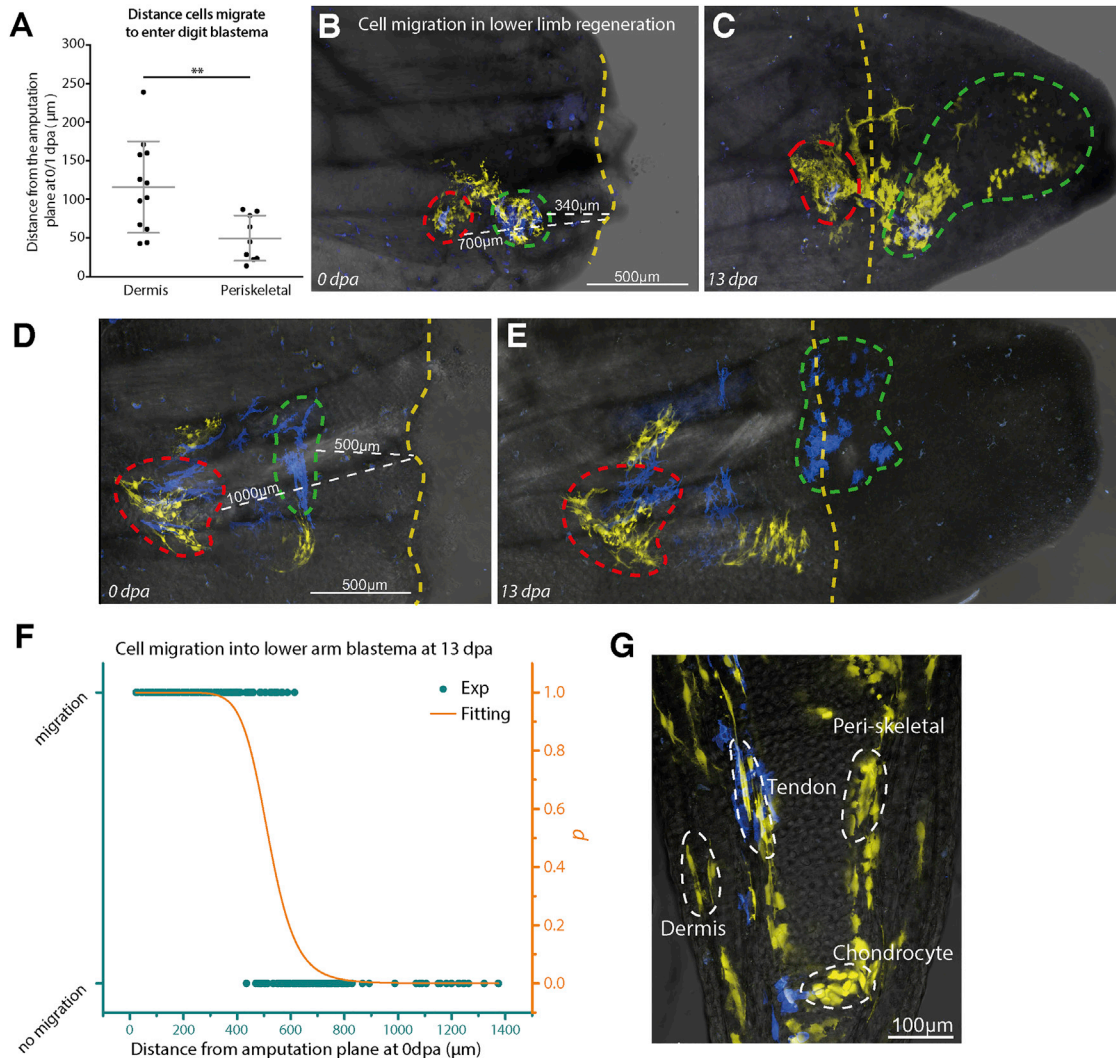
Figure 5. Definable Source Zones of Blastema Cells

(A) Time-lapse data of digit tip regeneration were used to retrospectively determine the distance from which dermal and periskeletal cells had traveled to enter the blastema. Dermal cells traveled from a larger source zone (average 116 μm, SD = 59 μm) than periskeletal cells (average 50 μm, SD = 29 μm) (n = 21 cells, n = 4 animals; **p = 0.007, Mann-Whitney nonparametric). Error bars represent SD.

(B–G) Determining the source zone of dermally associated connective tissue cells in lower limb regeneration. (B and D) Two examples of Limbow skin grafts that were used to label surface dermally associated cells. After amputation, the nearest distance (indicated by white dashed lines) to the amputation plane (yellow dashed line) was calculated for single cells or cohorts of cells (green and red dashed lines). Images were taken at regular intervals and it was determined whether cells had entered the blastema by 13 dpa (C and E). (F) Individual cells (green dots) were categorized by whether or not they entered the blastema by 13 dpa and plotted according to their starting distance from the amputation plane at 0 dpa. The normalized distance distributions of the migrating and nonmigrating cells were used to calculate a probability of migration (*p*, Figure S5; see Experimental Procedures). Fitting by a Hill function (orange line) yielded a distance of 518 μm as the source zone of lower arm dermal cells (see Figure S5C). (G) Dermally associated connective tissue cells from Limbow skin grafts contribute to tendons, cartilage, periskeletal, and dermal fibroblasts in the regenerated host digits at 90 dpa.

See also Figure S5.

PD mean distance of the clone relative to the amputation was used. The final cell types produced by the cell are denoted by the colored circles at the end of the track. In addition, we provide lineage trees of a number of cells in Figure S4A. During early blastema formation stages the first migration of periskeletal cells across the face of the severed skeleton was observed between 3 and 5 dpa (Figures 3A and 3D). Figure S2A shows daily images of this event. These cells integrated into the nascent cartilage core

and formed proliferative chondrocytes or periskeletal cells (Figure 3D). There were also early-migrating dermal cells that crossed the amputation plane prior to 8 dpa (see upper traces in Figure 3D). Compared with the early-migrating periskeletal cells, a number of the early dermal cells migrated a longer distance distally (Figures 3B and 3D). Similar to the periskeletal cells, these early-arriving dermal cells often integrated into the growing cartilage core.
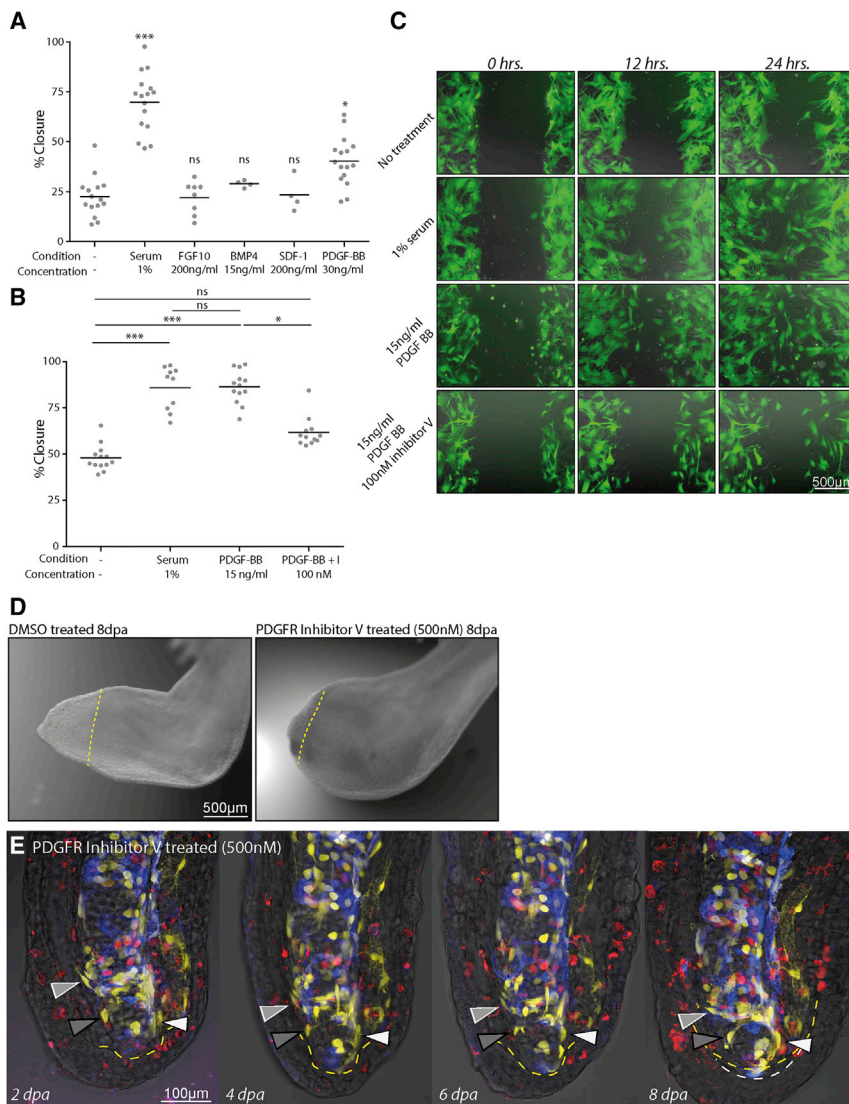
Figure 6. PDGF Signaling Is Required for Fibroblast Migration during Blastema Formation

(A) A primary screen implementing scratch wounds of GFP-labeled primary limb connective tissue blastema cell cultures (LPM GFP[+] blastema) to identify factors that enhance migration into scratch wounds over 48 hr (n = 1; *p < 0.05, ***p < 0.005; ns, nonsignificant; Kruskal-Wallis, Dunn's ad hoc nonparametric).

(B) Secondary screen of blastema cells confirms a promigratory effect of PDGF-BB on connective tissue migration within 24 hr of monolayer wounding that is repressed by addition of an inhibitor of PDGFR signaling (inhibitor V, CAS no. 347155-76-4) (n = 12, n = 3; *p < 0.05, ***p < 0.005; ns, nonsignificant; Kruskal-Wallis, Dunn's ad hoc nonparametric).

(C) Images of LPM GFP[+] blastema cell cultures at 0, 12, and 24 hr post wounding and treatment starting at 0 hr with 1% serum, 15 ng/mL PDGF-BB, or 15 ng/mL PDGF-BB + 100 nM PDGFR inhibitor V.

(D) Treatment of animals with 500 nM PDGFR inhibitor V (right panel) caused a block of lower arm regeneration at 8 dpa compared with DMSO-treated controls (left panel). Yellow dashed lines indicate the amputation plane.

(E) PDGFR inhibitor treatment blocks migration of dermal blastema progenitors beyond the amputation plane. Images from time course of digit regeneration in the presence of PDGFR inhibitor shows lack of fibroblast migration (white, light gray, dark gray arrowheads). Amputation plane is indicated by yellow dashed lines while white dashed lines indicate the mesenchymal blastema. See also Figure S6 and, for control regeneration at 8 dpa, see Figure S6E.

Late Waves of Dermal Fibroblast Migration Regenerate Soft Connective Tissue

Unlike periskeletal cells, dermal fibroblast migration continued beyond the early phase, crossing the amputation plane over a broad range of times after amputation. Cells entering the blastema close to and during the middle phase (9–11 dpa) consequently contributed to regenerating cartilage (Figures 3B, 3D, and S2B) as well as the distal soft connective tissue (Figure 3C, white arrowheads). Dermal fibroblasts that entered the blastema during the late phase (12–18 dpa) did not reach the distal regions of the regenerate and ultimately contributed to soft connective tissue in lateral regions of the regenerate (Figures 3C [gray arrowhead] and 3D). When we examined 22 cells (12 dermal, 10 periskeletal, from four animals), the time at which the cell entered the blastema corresponded to whether it was likely to form a skeletal (cartilage) cell or a soft connective tissue cell (Figure 3E). The late-migrating cells generally represented those cells that had originated further back from the amputation plane compared with early-

entering cells, although occasionally a fast-migrating cell from a distant region could enter the blastema early (Figure 3D). These results illustrate a correspondence between a cell's distance from the amputation plane, its timing of migration into the blastema, and its contribution to different compartments of the regenerated digit tip.

Clone Sizes

We never observed proliferation of periskeletal cells or dermal fibroblasts before cells had already migrated to the amputation plane or into the blastema (earliest events observed were 3–5 dpa, Figure S4A). Blastema clones were likely to undergo at least two divisions, often within 48–72 hr of each other (Figures 4A, 4B, and S4A). Based on single cells that were traced over the course of digit regeneration, we were able to quantify the distribution of clone sizes. Soft connective tissue-derived blastema cells such as periskeletal and dermal fibroblasts gave rise to clones with a mean size of 4.5 cells (n = 33, Figure 4C). These clone sizes were observed regardless of the final outcome of cells, suggesting that there was relatively even proliferative potential of blastema cells.

Quantifiable Source Zones of Connective Tissue Progenitors for Regeneration

We next sought to determine whether there was a definable "source zone" within mature tissue from which cells are recruited to the blastema. Since cell migration constituted a large part of building the blastema, this zone would primarily define the spatial extent of activated cell migration. In the digit tip, it was straightforward to track cells and determine their starting position. Given the significant contribution of periskeletal and dermal cells to digit regeneration, we focused on analyzing these two cell types. There was a clear difference in the distance with respect to the amputation plane from which dermal and periskeletal cells migrated. Periskeletal cells originated from a mean distance of 49 μm (SD 29 μm, n = 9) behind the amputation plane (Figure 5A). Dermal cells migrated on average from 116 μm (SD 59 μm, n = 12) behind the amputation plane to enter the blastema (Figure 5A). This indicates that there is indeed a source zone from which cells are recruited, and that the source zone varies depending on the cell type.

We next wanted to determine whether some of our observations in the digit tip were comparable with full limb regeneration. To address this question, we grafted a patch (~200–500 μm²) of recombined Limbow full-thickness skin from the ventral lower arm onto the same region of a nontransgenic host limb and allowed healing for 2 weeks until no physical junction of the graft was apparent. By varying the amputation injury in relation to the graft we were able to determine the distance from which the grafted cells migrate into the blastema. We found that within a 0- to 500-μm zone (518 μm calculated value, see Experimental Procedures), cells changed their morphology and migrated into the blastema (Figures 5B–5F and S5). The connective tissue cells within the dermal graft were highly migratory and gave rise to all of the connective tissue compartments in the regenerated digit tip with the exception of pericytes (Figure 5G). These limb tracings also confirmed that labeled pericytes began migration at later times and retained a tight association with blood vessels (Figures S3D–S3F). Thus, the source zone for lower limb regeneration was defined as approximately 500 μm.

PDGF Is an Activator of Fibroblast Migration that Is Essential for Blastema Formation

Because cell migration was a dominant, early feature of blastema formation, we searched for extracellular signals that activate connective tissue cell migration. We established conditions for primary culture of limb connective cells (see Supplemental Experimental Procedures). To verify that these cultures were composed of connective tissue, we derived cells from GFP LPM-transplanted animals and identified culture conditions that favored propagation of GFP⁺ cells (Figure 6C). These primary cultures could be passaged and they retained proliferative and migratory capacity in culture. We observed that after making a 0.9-mm scratch, cells would migrate rapidly to close the scratch in the presence of 1% serum compared with no serum (Figure 6C). To test candidates for "motogenic" effects, we used our ex vivo scratch-wound assay under no-serum conditions. We picked candidates that had been implicated as chemotactic growth factors involved in wound healing or regeneration to perform an initial screen. This candidate list included factors whose expression increases early after amputation (FGF10, BMP2/4, SDF-1, PDGF-BB), and serum proteins ex-

pected to be present at the wound site (PDGF-BB, BMP2/4) (Clunn et al., 1997) (Knapp et al., 2013) (Stewart et al., 2013). Among several candidates tested in this initial experiment, PDGF-BB induced increased migration of cells over medium alone (Figure 6A). Retesting of PDGF at several concentrations showed that 15 ng/mL had a potent stimulatory effect on migration, comparable with the serum-positive control (Figures 6B and 6C). Furthermore, cells treated with a specific inhibitor of PDGFR tyrosine kinase activity at 100 nM (PDGFR inhibitor V, CAS no. 347155-76-4) (Furuta et al., 2006) failed to close ex vivo scratch wounds (Figures 6B and 6C).

Having identified a motogenic factor ex vivo, we tested whether it indeed played a role in vivo in regeneration. Previous expression profiling showed that *Pdgf-b* and *Pdgfrβ* increased expression as early as 3–6 hr post amputation, reaching a maximum at 1–3 dpa. *Pdgfrα*, on the other hand, increased only at late stages, after 15 dpa (Figure S6A) (Stewart et al., 2013). We therefore asked whether *Pdgf-b* and *Pdgfrβ* were present in the mesenchymal blastema or wound epidermis using in situ hybridization (Figures S6B and S6C). Upper limb blastemas were used to create a larger number of cells for analysis, which gave more confidence in the results. *Pdgf-b* was expressed in the mesenchymal blastema and not the wound epidermis (Figure S6B). We also observed expression of *Pdgfrβ* in the mesenchymal blastema and not the wound epidermis (Figure S6C). To confirm that connective tissue cells express the receptor, we performed the in situ hybridization on sections from a GFP LPM-labeled limb, and immunostained the sections for GFP (Figures S6D and S6D′). We observed extensive colocalization of the in situ signal with the GFP signal at the cellular level (Figure S6D′, arrowheads), confirming that connective tissue cells express the receptor and would be a primary responder to the PDGF-B released from platelets and blastema cells. The LPM transplant often does not label 100% of limb connective tissue depending on the size and location of the final grafted piece. Therefore *Pdgfr*-positive, GFP-negative blastema cells are expected.

To functionally test the requirement of PDGF signaling on blastema formation, we treated amputated lower limbs with 500 nM PDGFR inhibitor, which caused a complete block of lower limb blastema formation as assessed by whole-mount bright-field imaging (Figure 6D). We then examined the effect of PDGF signaling inhibition in the digit tip where we could resolve the effect of drug treatment on single cells. When digits were treated with PDGFR inhibitor prior to and during regeneration, epidermal wound healing remained active; however, we observed inhibition of dermal fibroblast migration into the blastema, and consequently a lack of blastema formation (Figure 6E). Interestingly, treatment of already formed blastemas with the inhibitor did not perturb blastema growth or morphogenesis, indicating that inhibition of PDGF specifically affects cell migration into the blastema (Figures S6E and S6F). Thus, PDGF signaling is vital for connective tissue cells to migrate beyond the amputation plane, an essential first step in creating the blastema.

DISCUSSION

The process of blastema formation has previously suffered from a paucity of knowledge of which cells found the blastema and how they found the blastema; for example, via selection and expansive asymmetric proliferation or via wholesale tissue
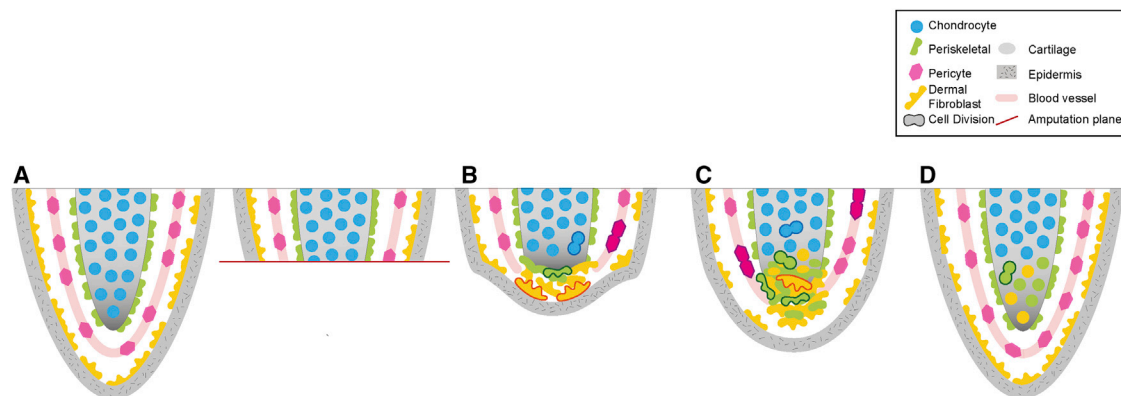
Figure 7. Schematic Summary of Connective Cell Contributions and Dynamics during Digit Regeneration
(A) The digit starts as an intact tissue with various connective tissue subcompartments. Chondrocytes, blue; pericytes, pink; periskeletal cells, green; dermal fibroblasts, orange.
(B) At the early stage after amputation, chondrocytes proliferate in situ and remain in place. Pericytes also divide behind the amputation plane. Periskeletal cells migrate without cell division across the surface of the skeleton, while dermal cells migrate underneath the wound epidermis (gray).
(C) In the mid-phase of regeneration, pericyte cells migrate along blood vessels into the blastema but retain their identity. Early-migrating periskeletal cells and dermal cells start proliferating, often already within the newly forming cartilage core. Migration of other periskeletal and dermal cells from behind the amputation plane continues.
(D) In the late phase of migration, tissue boundaries are already visible and late-migrating dermal cells contribute to lateral soft connective tissue.

migration. Our live imaging of connective tissue cells at single-cell resolution during axolotl digit regeneration has provided some important insight into how the blastema forms (Figure 7).

We found that not all connective tissue cell types are equal. After amputation, chondrocytes divide but do not contribute to the regenerate. Previous tracking experiments all relied on transplantation of marked cells into regenerating limbs, accessory limbs, or irradiated hosts. Some of these transplantation studies suggested that chondrocytes contribute significantly to the regenerate (Cameron and Hinterberger, 1984), whereas others suggested limited participation in regeneration (McCusker et al., 2016; Muneoka et al., 1986). Here we tracked cells in situ during regeneration to assess the contribution of chondrocytes. These results show that chondrocytes are susceptible to proliferative cues emanating from the amputation plane but retain differentiated morphology and position. These results question the relevance of strategies to promote cartilage regeneration by enhancing chondrocyte proliferation.

Our work also represents the first description of pericyte fate during axolotl appendage regeneration and shows that the pericyte is not a major contributor to skeleton or other cell types and skeleton in digit regeneration. The limited regenerative potential of pericyte cells is interesting in the context of mammalian studies. These studies have suggested that mammalian pericytes can dissociate from blood vessels to form fibroblastic, chondro-osteogenic, or even muscle cells, depending on their tissue of origin (Dellavalle et al., 2007; Sacchetti et al., 2007). The different observations between the axolotl and mammalian systems could have several bases. The axolotl pericytes that were tracked here derive solely from LPM. Several observations suggest that pericytes could have multiple embryonic origins, although LPM is considered a primary source of pericytes (Cappellari et al., 2013; Cappellari and Cossu, 2013). In the mammalian studies, the pericytes that display multipotent phenotypes may represent a small-minority fraction of the total population

(Sacchetti et al., 2016). Here we have described the fate of pericytes using cell tracking of clones in which we could account for every descendant that was produced during regeneration. There is a small possibility that there were clones in which a cell wandered off the blood vessel between time points and was lost to tracking. However, our observation of isolated, clonal pericytes in the lower limb transplants suggests that our pericytes remain firmly associated with blood vessels during regeneration. A last possibility is that cognate axolotl and mammalian pericytes truly show differences in cell potential. In any case, our data definitively show that a highly multipotent pericyte is not a major, integral contributor to digit regeneration.

In the axolotl digit, the building of new cartilage is largely the responsibility of periskeletal cells and dermal fibroblasts. The two cell types were recruited from differently sized zones behind the amputation plane showing a divergence in mechanism, although they both contribute to cartilage in the end. We have defined the source zone for regeneration in three contexts: periskeletal cells in digit regeneration, dermal cells in digit regeneration, and dermally associated cells in lower limb regeneration. This indicates that the different contexts yield different magnitudes of distance in which initial cues for migration act. This knowledge will be important for identifying molecular regulators whose action or distribution correspond to these defined zones and for understanding how their molecular range of action is controlled.

One unanswered question relates to the heterogeneity of periskeletal cells. We did not address whether these cells represent a single cartilage-forming population or a mixture of committed cell types that are poised to contribute to cartilage and later stages of bone formation that were not visualized in these experiments. In some regenerative contexts, cells retain a dual identity, displaying aspects of both osteo- and chondroprogenitors (Paul et al., 2016).

Our data suggest that the timing of entry into the blastema has an influence on the eventual fate and spatial location that a

dermal cell adopts during regeneration. Early-entering cells often became cartilage cells whereas late-entering cells never reached the distal core of the regenerate and were relegated to lateral soft connective tissue. Therefore, the time and location of migration choreographs cell fate in the blastema. A missing piece in the spatial coordination of limb connective tissue is the interstitial and fascia of the muscle, which are not present in the digit tip. We hypothesize that these cells should have a major role in skeleton formation, perhaps more so than dermal fibroblasts, due to their closer proximity to the stump skeleton. Transgenic lineage tracing will be an important step in isolating the contributions of this tissue compartment.

Our data would suggest that cells poised with a higher migratory potential will be selected for the early blastema. Cell tracking in lower limb amputations revealed that in such a context a large proportion of dermally associated cells next to the amputation can enter the blastema, indicating that regeneration does not select a very rare stem cell but recruits a significant fraction of periskeletal cells and dermal fibroblasts adjacent to the amputation plane into the blastema.

Corresponding to migration having an important role in blastema establishment, we identified PDGF signaling as being required for connective tissue cell migration and onset of blastema formation. This treatment did not prevent the growth of already formed blastemas, suggesting that PDGF signaling is specifically implemented to promote migration of cells into the blastema. In vertebrates, PDGFRs are broadly expressed in interstitial stromal cells, and PDGF can act as a directional chemoattractant on cultured mammalian fibroblasts (Seppa et al., 1982) (Andrae et al., 2008). The role of PDGF as a chemoattractant in vivo has been most clearly delineated in *Xenopus* embryonic gastrulation (Nagel et al., 2004). The digit regeneration system described here has provided, for the first time, a clear link between an ex vivo fibroblast migration assay and in vivo fibroblast migration required for tissue regeneration. Since PDGF is delivered by platelets to wound sites (Antoniades et al., 1979), it is likely distributed over the entire wound site.

Connective tissue fibroblasts in human injuries are associated with fibrosis and scarring, while in axolotl these cells are the main actors in a pro-regenerative response that rebuilds skeletal structure. Our work here has provided the foundational knowledge to track and understand the pro-regenerative behaviors of fibroblasts that may be used in future to divert human fibroblasts from a scarring phenotype to a regenerative one.

EXPERIMENTAL PROCEDURES

Animal Husbandry, Transgenesis, and Embryonic and Larval Surgeries

To create brainbow transgenic axolotls, we subcloned the Brainbow 2.1 cassette (Livet et al., 2007) into a plasmid containing the ubiquitous CAGGs promoter and flanked with SceI meganuclease sites. Fertilized embryos from nontransgenic animals were injected with brainbow construct and SceI as previously described (Khattak et al., 2014). Transgenic founders were allowed to grow to sexual maturity and F1 progeny were screened for brightness, penetrance, and stability of transgene expression by the default nuclear hrGFPII expression and also after recombination. Double transgenic animals were created by breeding Brainbow animals to an already established CAGGs:: ERT-Cre-ERT-T2A-GFPnls line (Khattak et al., 2013). Double transgenic animals from the initial breeding and subsequent F1 double transgenic animals were used as donors for embryonic transplantation and clonal analysis.

Embryonic transplantation of LPM from double transgenic animals onto nontransgenic hosts was performed as previously described (Kragl et al., 2009). Transplant host animals (i.e., Limbow) were screened after limb formation for faithful labeling of only connective tissue compartments in limbs and digits. Once limb morphogenesis had completed and digits contained the full complement of segments (3–3.5 cm body length), recombination was induced by bathing in tap water containing (Z)-4-hydroxytamoxifen (Sigma) at concentrations ranging from 100 nM to 2 μM for a duration of 30 min to overnight to vary the degree of recombination (Khattak et al., 2014). Afterward, the animals were washed and screened for 2 weeks to ensure fluorescent color stability. All experiments were done in accordance with the Saxony Animal Ethics Committee.

Axolotl Live Imaging

For imaging of recombined Limbow animals, animals were anesthetized with 0.007% benzocaine solution and mounted on a glass-bottomed chamber (Willco) with sufficient liquid to maintain them for durations of more than 20 min. Animals were imaged on a Zeiss confocal laser scanning microscope LSM 780 Axio Observer of the Light Microscopy Facility, a core facility of BIOTEC/CRTD at Technische Universität Dresden. Image stacks were acquired every 24 hr for 18–24 days following amputation of the digit.

Image Processing and Cell Tracking

After acquisition, each channel of the image stack was manually aligned to account for sample movement during imaging. Image stacks over the time course of regeneration were concatenated into a multidimensional stack and manual cell tracking was performed using the Fiji plugin Trackmate. Tracking cells from sequential time points was verified by measuring fluorescent intensities of cells of interest and neighboring clones using Fiji and Photoshop. Only cells with distinct color intensities and that could be tracked from 1 dpa through the 18-day course of regeneration were used for analysis. Other parameters of tracked cells such as fluorescent intensity and distance to the amputation plane were measured using Fiji and exported to Prism (GraphPad) for statistical tests and visualization.

For presentation of images herein, channel-specific contrast enhancements were undertaken to aid in visualization of complex, multicolor image stacks. All processing steps were applied equally to the entire micrograph field of a given channel. Bright-field images of nonfluorescent tissue were overlaid on Limbow images with an altered opacity to show structures without obscuring fluorescent visualization. All images represent maximum-intensity projections of subsets of the total image volume to highlight specific tracked cells.

Statistics

Data were compared by nonparametric tests (i.e., without assuming normally distributed data). The Kruskal-Wallis test followed by the post hoc Dunn test was used for multiple comparisons and the Mann-Whitney test for paired comparisons.

Calculation of the Space-Dependent Probability of Migration into the Blastema

Grafted dermal progenitors were categorized in terms of whether they migrated into the blastema at 13 dpa or not (Figure S5A). The histogram of cell distances from the amputation plane at 0 dpa was plotted for the two categories (Figure S5B, columns). This was used to determine a frequency for each distance, x, of whether a cell would enter ($f_e(x)$) or not ($f_n(x)$) into the blastema at 13 dpa. From adding both histograms (Figure S5B, dashed line), the normalized quantity $p(x) = f_e(x)/[f_e(x) + f_n(x)]$ was calculated, which estimates the probability of finding a cell entering into the blastema at 13 dpa at the distance x from the amputation plane (Figure S5C, dots). This probability distribution was fitted (Figure S5C, continuous curve) with the following Hill-like expression by means of a least-square minimization algorithm:

$$p(x) = \frac{1}{1 + \left(\frac{x_{50}}{x}\right)^h},$$

where x_{50} represents the distance to the amputation plane in which the probability of migration into the blastema at 13 dpa is 50%, while h is a measure of the sigmoidicity.

Axolotl Ex Vivo Scratch-Wound Assay

LPM GFP$^+$ Blastema cultures were seeded at a confluency of 3×10^4 cells/well on 24-well plates precoated with fibronectin from bovine plasma (33.3 μg/mL, Sigma) and serum starved for 36 hr. Two perpendicular scratches were introduced in each well by scraping the cell monolayer with a white (10 μL) or a yellow (200 μL) sterile pipette tip. After washing with serum-free medium, the respective treatments were performed: base culture medium, culture medium with 1× supplements (1% serum), or base culture medium with different growth factors or inhibitors (PDGFR inhibitor V [CAS no. 347155-76-4, Merck Millipore]). Treatments were added at 0 hr and 24 hr at indicated concentrations. Between two and five random fields in each scratch were manually chosen for quantification. Phase-contrast/fluorescent images of these fields were captured at indicated time points using a 5× objective and an AxioObserver microscope (Zeiss). For additional information, see Supplemental Experimental Procedures.

SUPPLEMENTAL INFORMATION

Supplemental Information includes Supplemental Experimental Procedures, six figures, and one movie and can be found with this article online at http://dx.doi.org/10.1016/j.devcel.2016.10.013.

REFERENCES

Andrae, J., Gallini, R., and Betsholtz, C. (2008). Role of platelet-derived growth factors in physiology and medicine. Genes Dev. 22, 1276–1312.

Antoniades, H.N., Scher, C.D., and Stiles, C.D. (1979). Purification of human platelet-derived growth factor. Proc. Natl. Acad. Sci. USA 76, 1809–1813.

Bryant, S.V., Endo, T., and Gardiner, D.M. (2002). Vertebrate limb regeneration and the origin of limb stem cells. Int. J. Dev. Biol. 46, 887–896.

Cameron, J.A., and Hinterberger, T.J. (1984). Regional differences in the distribution of myogenic and chondrogenic cells in axolotl limb blastemas. J. Exp. Zool. 232, 269–275.

Cappellari, O., and Cossu, G. (2013). Pericytes in development and pathology of skeletal muscle. Circ. Res. 113, 341–347.

Cappellari, O., Benedetti, S., Innocenzi, A., Tedesco, F.S., Moreno-Fortuny, A., Ugarte, G., Lampugnani, M.G., Messina, G., and Cossu, G. (2013). Dll4 and PDGF-BB convert committed skeletal myoblasts to pericytes without erasing their myogenic memory. Dev. Cell 24, 586–599.

Carlson, B.M. (1974). Morphogenetic interactions between rotated skin cuffs and underlying stump tissues in regenerating axolotl forelimbs. Dev. Biol. 39, 263–285.

Clunn, G.F., Refson, J.S., Lymn, J.S., and Hughes, A.D. (1997). Platelet-derived growth factor beta-receptors can both promote and inhibit chemotaxis in human vascular smooth muscle cells. Arterioscler. Thromb. Vasc. Biol. 17, 2622–2629.

Dellavalle, A., Sampaolesi, M., Tonlorenzi, R., Tagliafico, E., Sacchetti, B., Perani, L., Innocenzi, A., Galvez, B.G., Messina, G., Morosetti, R., et al. (2007). Pericytes of human skeletal muscle are myogenic precursors distinct from satellite cells. Nat. Cell Biol. 9, 255–267.

Dunis, D.A., and Namenwirth, M. (1977). The role of grafted skin in the regeneration of x-irradiated axolotl limbs. Dev. Biol. 56, 97–109.

Furuta, T., Sakai, T., Senga, T., Osawa, T., Kubo, K., Shimizu, T., Suzuki, R., Yoshino, T., Endo, M., and Miwa, A. (2006). Identification of potent and selective inhibitors of PDGF receptor autophosphorylation. J. Med. Chem. 49, 2186–2192.

Gardiner, D.M., Muneoka, K., and Bryant, S.V. (1986). The migration of dermal cells during blastema formation in axolotls. Dev. Biol. 118, 488–493.

Khattak, S., Schuez, M., Richter, T., Knapp, D., Haigo, S.L., Sandoval-Guzman, T., Hradlikova, K., Duemmler, A., Kerney, R., and Tanaka, E.M. (2013). Germline transgenic methods for tracking cells and testing gene function during regeneration in the axolotl. Stem Cell Rep. 1, 90–103.

Khattak, S., Murawala, P., Andreas, H., Kappert, V., Schuez, M., Sandoval-Guzman, T., Crawford, K., and Tanaka, E.M. (2014). Optimized axolotl (Ambystoma mexicanum) husbandry, breeding, metamorphosis, transgenesis and tamoxifen-mediated recombination. Nat. Protoc. 9, 529–540.

Knapp, D., Schulz, H., Rascon, C.A., Volkmer, M., Scholz, J., Nacu, E., Le, M., Novozhilov, S., Tazaki, A., Protze, S., et al. (2013). Comparative transcriptional profiling of the axolotl limb identifies a tripartite regeneration-specific gene program. PLoS One 8, e61352.

Kragl, M., Knapp, D., Nacu, E., Khattak, S., Maden, M., Epperlein, H.H., and Tanaka, E.M. (2009). Cells keep a memory of their tissue origin during axolotl limb regeneration. Nature 460, 60–65.

Livet, J., Weissman, T.A., Kang, H., Draft, R.W., Lu, J., Bennis, R.A., Sanes, J.R., and Lichtman, J.W. (2007). Transgenic strategies for combinatorial expression of fluorescent proteins in the nervous system. Nature 450, 56–62.

McCusker, C.D., Diaz-Castillo, C., Sosnik, J., Q Phan, A., and Gardiner, D.M. (2016). Cartilage and bone cells do not participate in skeletal regeneration in Ambystoma mexicanum limbs. Dev. Biol. 416, 26–33.

Monaghan, J.R., Epp, L.G., Putta, S., Page, R.B., Walker, J.A., Beachy, C.K., Zhu, W., Pao, G.M., Verma, I.M., Hunter, T., et al. (2009). Microarray and cDNA sequence analysis of transcription during nerve-dependent limb regeneration. BMC Biol. 7, 1.

Muneoka, K., Fox, W.F., and Bryant, S.V. (1986). Cellular contribution from dermis and cartilage to the regenerating limb blastema in axolotls. Dev. Biol. 116, 256–260.

Nacu, E., Glausch, M., Le, H.Q., Damanik, F.F., Schuez, M., Knapp, D., Khattak, S., Richter, T., and Tanaka, E.M. (2013). Connective tissue cells, but not muscle cells, are involved in establishing the proximo-distal outcome of limb regeneration in the axolotl. Development 140, 513–518.

Nagel, M., Tahinci, E., Symes, K., and Winklbauer, R. (2004). Guidance of mesoderm cell migration in the Xenopus gastrula requires PDGF signaling. Development 131, 2727–2736.

Paul, S., Schindler, S., Giovannone, D., de Millo Terrazzani, A., Mariani, F.V., and Crump, J.G. (2016). Ihha induces hybrid cartilage-bone cells during zebrafish jawbone regeneration. Development 143, 2066–2076.

Rodrigo Albors, A., Tazaki, A., Rost, F., Nowoshilow, S., Chara, O., and Tanaka, E.M. (2015). Planar cell polarity-mediated induction of neural stem cell expansion during axolotl spinal cord regeneration. Elife 4, e10230.

Rollman-Dinsmore, C., and Bryant, S.V. (1982). Pattern regulation between hind- and forelimbs after blastema exchanges and skin grafts in Notophthalmus viridescens. J. Exp. Zool. 223, 51–56.

Sacchetti, B., Funari, A., Michienzi, S., Di Cesare, S., Piersanti, S., Saggio, I., Tagliafico, E., Ferrari, S., Robey, P.G., Riminucci, M., et al. (2007). Self-renewing osteoprogenitors in bone marrow sinusoids can organize a hematopoietic microenvironment. Cell 131, 324–336.

Sacchetti, B., Funari, A., Remoli, C., Giannicola, G., Kogler, G., Liedtke, S., Cossu, G., Serafini, M., Sampaolesi, M., Tagliafico, E., et al. (2016). No identical "mesenchymal stem cells" at different times and sites: human committed progenitors of distinct origin and differentiation potential are incorporated as adventitial cells in microvessels. Stem Cell Rep. 6, 897–913.

Sandoval-Guzman, T., Wang, H., Khattak, S., Schuez, M., Roensch, K., Nacu, E., Tazaki, A., Joven, A., Tanaka, E.M., and Simon, A. (2014). Fundamental differences in dedifferentiation and stem cell recruitment during skeletal muscle regeneration in two salamander species. Cell Stem Cell 14, 174–187.

Seppa, H., Grotendorst, G., Seppa, S., Schiffmann, E., and Martin, G.R. (1982). Platelet-derived growth factor in chemotactic for fibroblasts. J. Cell Biol. 92, 584–588.

Stewart, R., Rascon, C.A., Tian, S., Nie, J., Barry, C., Chu, L.F., Ardalani, H., Wagner, R.J., Probasco, M.D., Bolin, J.M., et al. (2013). Comparative RNA-seq analysis in the unsequenced axolotl: the oncogene burst highlights early gene expression in the blastema. PLoS Comput. Biol. 9, e1002936.

Tanaka, E.M. (2016). The molecular and cellular choreography of appendage regeneration. Cell 165, 1598–1608.